Pure rutile nanotubes

Dominik Eder,* Ian A. Kinloch and Alan H. Windle

Received (in Cambridge, UK) 7th December 2005, Accepted 2nd February 2006
First published as an Advance Article on the web 23rd February 2006
DOI: 10.1039/b517260h

We present a novel method to produce pure rutile nanotubes using a sacrificial carbon nanotube template.

Titania (TiO_2), which is one of the most widely used transition metal oxides, has two main phases, anatase which can be kinetically favoured over rutile, the thermodynamically stable phase.[1] Applications for titania include photo-electrochemical splitting of water,[2,3] photo-degradation of organic molecules for purifying water and air,[4,5] dye-sensitised solar cells[6] and catalyst supports.[7] The fabrication of nanoporous and especially nano-structured titania is thus a key challenge. Titania nanotubes and nanofibrils have the advantage that they can be used to form three-dimensional mechanically coherent architectures, which provide ready gas access to a high surface area.[8] Titania nanotubes have already been used in some applications[9,10] however their structures have been either anatase or a TiO_x polymorph.[11,12] Such tubes were produced by hydrothermal treatment of TiO_2 with NaOH at temperatures between 110 °C and 150 °C,[13] anodic oxidation of titanium foils[14] or a sol–gel process[15] using either alumina,[16] cholesterol-based aggregates[17] or carbon nanotubes[18] as templates. A specific attempt to change anatase into rutile nanotubes by heating found that the tube morphology collapsed with loss of structural control.[14] Hitherto there are no reports on successful synthesis of titania nanotubes in the pure rutile phase.

There is strong evidence that rutile would be the favoured form of titania for nanotubes in terms of: selectivity and improved kinetics in photo-catalytic reactions,[1,19] dielectric constant[7,20] and refractive index (2.9 for rutile *versus* 2.4 for anatase) for photo-electronic applications.[21] For example, it has been reported recently that rutile crystals smaller than 10 nm show comparable, if not higher, photo-catalytic activity than anatase.[22] However, these crystals were found to increase in size at the higher temperatures necessary for some applications, thus changing the photo-chemical properties.[23] Also, the photo-catalytic activity of TiO_2 for the decomposition of ozone[24] as well as for the photo-catalytic degradation of organic sulfides[25] increases in the order: anatase, anatase–rutile mixture, rutile. A possible explanation for the preference of rutile in these photo-chemical reactions is that the bandgap for rutile is smaller than anatase by 0.2 eV (the bandgap can of course be modified further through doping of titania by nitrogen or sulfur). The best catalyst for the production of hydrogen from biomass reformation is reported to be ruthenium supported on rutile.[26] Electronic devices[27,28] is another area where rutile is preferred due to its very high dielectric constant ($\varepsilon \sim 90$–100) compared to anatase ($\varepsilon \sim 30$–40).[7] In future, nanostructured rutile might also replace today's sapphire as a dielectric resonator in high-stability oscillators in satellites or atomic clocks.[29] In the upcoming field of photonic crystals, materials with a "complete bandgap" are needed, for which a refractive index of at least 2.9 is necessary,[21,30] a value which can only be achieved by the rutile form.

We report here a method for the production of pure rutile nanotubes involving the sol–gel route which uses carbon nanotubes as templates, with subsequent heat treatment being used to convert the templated anatase to rutile. A key aspect of this method is that the carbon nanotubes support the structure during the anatase–rutile reconstructive phase transformation, preventing break up as a result of transformation stresses. The carbon templates can be subsequently burnt-out to leave pure rutile nanotubes. Further advantages of this method are that the templates can be used to control the internal diameter of the rutile nanotubes, while synthesis conditions control the wall thickness.

The crystal structure of the samples was obtained by X-ray diffraction (XRD) using a Philips Expert PW3020 diffractometer (Cu-K_α radiation, 40 kV and 40 mA, λ = 1.5406 nm). The morphology was studied by high resolution scanning electron microscopy (JEOL 6340F FEG-SEM). For scanning electron microscopy (SEM) analysis, a thin layer of platinum was sputtered onto the surface of the samples to reduce charging effects. Transmission electron microscopy (TEM) was also used to examine the microstructure (JEOL 200CX).

The production route for the rutile nanotubes involved four processing stages: (1) coating of the carbon nanotubes with amorphous titania through a sol–gel process, (2) heating in air to convert the titania to anatase, (3) heating in nitrogen to transform the anatase to predominantly rutile and (4) heating in air again but at a higher temperature to remove the carbon nanotubes and to transform the remaining anatase.

The multi-walled carbon nanotubes were prepared by a modified chemical vapour deposition (CVD) process using ferrocene as catalyst precursor and toluene as the feedstock.[31] These reactants were vaporised into a hydrogen/argon atmosphere at 760 °C. Iron particles were produced by the decomposition from the ferrocene, which then acted as catalysts for the carbon nanotubes growth. The average outer diameter of the nanotubes was 70 nm and the length was between 20 and 30 μm. However, the dimensions of the nanotubes can be controlled by the reaction conditions.[31]

The carbon nanotubes were dispersed in ethanol with the aid of ultrasonication for 10 min. Benzylalcohol (BA) and water were then added and the solution stirred at 0 °C. Tetrabutyloxytitanate (TBOT) was dissolved in ethanol and slowly dropped into the CNT suspension, so that the final molar ratio was 1 : 3 : 6 : 30 (TBOT : BA : H_2O : ethanol). The concentration of the carbon

Department of Materials Science and Metallurgy, University of Cambridge, New Museums Site, Pembroke Street, Cambridge. E-mail: de235@cam.ac.uk; iak21@cam.ac.uk; ahw1@cam.ac.uk; Fax: +44 1223 334567; Tel: +44 1223 334300

nanotubes was calculated as the mass (wt%) related to the expected mass of the final TiO_2 coatings and varied between 1 and 50 wt%. Benzylalcohol was chosen due to its ability to act as a surface shaper, keeping the particle size low.[32] After one hour of stirring, the precipitate was filtered, washed in ethanol and dried in air at room temperature.

The filtered samples were found to consist of carbon nanotubes uniformly coated with titania, such that the outer diameter of the composite tubes was in the range of 60 to 250 nm. X-ray diffraction (XRD) studies revealed that this titania coating was amorphous (Fig. 1a).

Upon heating the samples in air at 400 °C for 2 h the titania crystallised completely into anatase (Fig. 1b), as was reported also by Jung *et al.*[17] The size of the anatase crystals was calculated to be 18–19 nm from the X-ray line width. The thickness of the coating depended on the concentration of the carbon nanotubes and the composition of the sol and ranged from 20 nm (high CNT loading) to 120 nm (low CNT loading) as obtained by SEM (Fig. 2A).

The samples were treated in flowing nitrogen with exclusion of oxygen for 4 h at temperatures between 700 °C and 900 °C, during which the anatase phase almost completely transformed into rutile (Fig. 1c) while preserving exactly the nanotube structure (Fig. 2B). Indeed, if the carbon is removed prior to the nitrogen heat treatment, then the tube morphology of the rutile is lost. The rutile nanotubes showed two types of morphology depending on the synthesis conditions. For thin anatase coatings, the nitrogen heat treatment produced a similarly smooth rutile coating (Fig. 3A). The electron diffraction pattern from these tubes was polycrystalline, with no preferred orientation. Rutile coatings produced from anatase coatings which were thicker than 50 nm consisted of an inner layer of smaller crystals, as previously described, and a semi-discrete outer layer of crystals 30 to 40 nm in size (Fig. 3B).

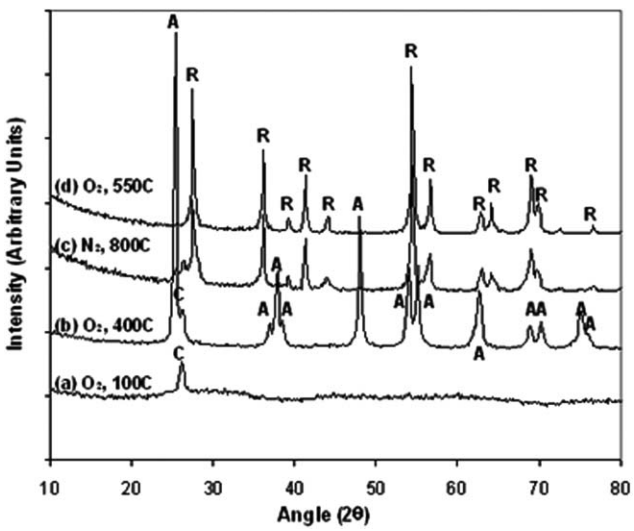

Fig. 1 X-ray diffraction scans obtained from titania coated carbon nanotubes: (a) directly after coating by the sol–gel process, (b) heated in air at 400 °C (crystallisation of anatase), (c) heat treated in nitrogen at 800 °C (phase transformation into rutile) and (d) heated in air at 550 °C (removal of the carbon nanotubes templates and total completion of transformation to rutile). The peaks labelled A, R and C are anatase, rutile and graphite respectively.

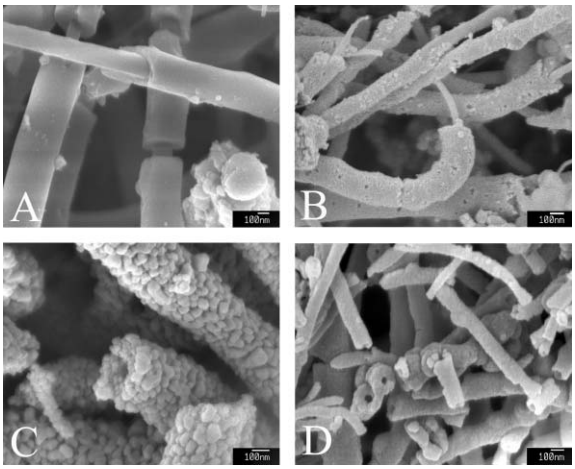

Fig. 2 SEM images of (A) carbon nanotubes coated with anatase, (B) carbon nanotubes coated predominantly with rutile as obtained after heat treatment in nitrogen at 800 °C, (C) thick rutile nanotubes with a rough coating after removing the template and (D) thin rutile nanotubes with a smooth coating after removing the template.

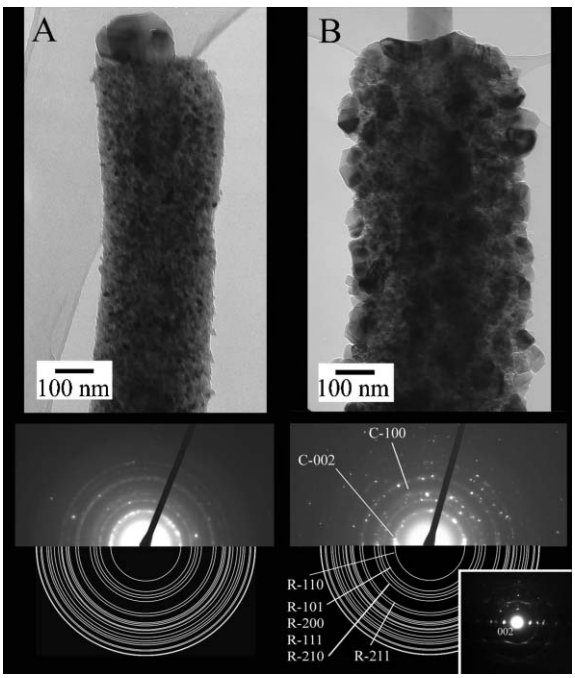

Fig. 3 TEM micrographs of carbon nanotubes coated with titania after heat treatment in nitrogen at 800 °C. (A) Shows the smooth rutile coating and (B) shows the thick coating which consists of the small crystal inner layer and the larger crystal outer layer. The top images are bright field, the lower images are the corresponding selected area electron diffraction patterns. The upper half of the diffraction pattern shows the experimental data while the lower half shows the rings calculated from the reference structure of rutile (labelled "R"). The diffraction from the carbon nanotubes is labelled "C". The inset in the lower image in (B) shows the reference diffraction pattern of the carbon nanotube template.

The final step in the process was the oxidation in air at 550 °C for 2 h to remove the carbon nanotubes. The oxidation temperature was carefully selected to be sufficiently high to oxidise the tubes but not so high as to destroy the rutile nanotube

morphology. These nanotubes were identified with XRD (Fig. 1d) and electron diffraction to be 100% rutile with no graphitic diffraction present. Interestingly, the temperature needed for this complete removal of carbon is significantly lower than that required to oxidise a pure nanotube sample (650 °C). The effect is still under detailed investigation but is believed to be due to a catalysing effect of the titania on the graphitic decomposition.

Fig. 2C and 2D show the nanotube morphology in the rutile after removal of the carbon nanotube template. The nanotubes were typically several microns long, with the length being limited to some extent by the cracking of the amorphous titania coating (Fig. 2A). The smooth rutile coating results in thin nanotubes with a wall thickness of 15 to 30 nm (Fig. 2C), while the rough coating produces thick nanotubes with a wall thickness between 40 and 120 nm (Fig. 2D). The specific surface area was measured by physisorption of nitrogen according to Brunauer-Emmett-Teller (BET) and ranges from 20 m^2g^{-1} for the thick nanotubes up to 70 $m^2\ g^{-1}$ for the thin tubes. Taken into account that for phase transformation the materials had already been treated at temperatures as high as 900 °C, the observed surface areas are quite large compared to nanopowders. For instance, Su *et al.* found that the BET surface area of anatase nanoparticles calcined at 700 °C for 2 h was only 11.5 m^2g^{-1}.[23] Furthermore, it is believed that the nanotubes will be able to produce architectures that can provide full access to their surface area, and current work is focussing in this direction.

Pure rutile nanotubes have been produced for the first time by using a carbon nanotube template for the deposition of an anatase coating, and subsequently to support it during the phase transformation to rutile. The carbon was then removed to leave rutile nanotubes. The process was followed using XRD and electron microscopy, with the final rutile crystal size depending on the initial thickness of the amorphous coating. Studies on the applications of these nanotubes to catalysis are currently being made.

Notes and references

1 O. Carp, C. L. Huisman and A. Reller, *Prog. Solid State Chem.*, 2004, **32**, 33–177.
2 A. Fujishima and K. Honda, *Nature*, 1972, **238**, 37.
3 S. U. M. Khan, M. Al-Shahry and W. B. Ingler, Jr., *Science*, 2002, **297**, 22–24.
4 M. R. Hoffmann, S. T. Martin, W. Choi and D. W. Bahnemann, *Chem. Rev.*, 1995, **95**, 69–96.
5 R. Asahi, T. Morikawa, T. Ohwaki, K. Aoki and Y. Yaga, *Science*, 2001, **293**, 269–271.
6 B. O'Regan and M. Graetzel, *Nature*, 1991, **353**, 737.
7 U. Diebold, *Surf. Sci. Rep.*, 2003, **48**, 53.
8 C. N. R. Rao and M. Nash, *Dalton Trans.*, 2003, **1**, 1–24.
9 O. K. Varghese, D. Gong, M. Paulose, K. G. Ong, E. C. Dickey and C. A. Grimes, *Adv. Mater.*, 2003, **15**, 7–8, 624.
10 M. Adachi, Y. Murata, I. Okada and S. Yoshikawa, *J. Electrochem. Soc.*, 2003, **150**, 8, G488–G493.
11 S. Zhang, Q. Chen and L. M. Peng, *Phys. Rev. B*, 2005, **71**, 014104–014115.
12 G. Armstrong, A. R. Armstrong, J. Canales and P. G. Bruce, *Chem. Commun.*, 2005, **21**, 19, 2454–6.
13 T. Kasuga, M. Hiramatsu, A. Hoson, T. Sekino and K. Niihara, *Adv. Mater.*, 1999, **11**, 15, 1307–1311.
14 O. K. Varghese, D. Gong, M. Paulose, C. A. Grimes and E. C. Dickey, *J. Mater. Res.*, 2003, **18**, 1, 156–165.
15 P. Yang, D. Zhao, D. I. Margolese, B. F. Chmelka and G. D. Stucky, *Nature*, 1998, **396**, 152.
16 H. Imai, Y. Takei, K. Shimizu, M. Matsuda and H. Hirahima, *J. Mater. Chem.*, 1999, **9**, 2971.
17 J. H. Jung, T. Shimizu and S. Shinkai, *J. Mater. Chem.*, 2005, **15**, 3979–3986.
18 J. Sun, L. Gao and Q. Zhang, *J. Mater. Sci. Lett.*, 2003, **22**, 339–341.
19 A. R. Gandhe, J. B. Fernandes, S. Varma and N. M. Gupta, *J. Mol. Catal. A: Chem.*, 2005, **238**, 1–2, 63–71.
20 D. Eder and R. Kramer, *J. Phys. Chem. B*, 2004, **108**, 39, 14823–29.
21 V. N. Manoharan, A. Imhof, J. D. Thorne and D. J. Pine, *Adv. Mater.*, 2001, **13**, 6, 447–450.
22 J. Sun, L. Gao and Q. Zhang, *J. Am. Ceram. Soc.*, 2003, **86**, 10, 1677–1682.
23 C. Su, B. Y. Hong and C. M. Tseng, *Catal. Today*, 2004, **96**, 119–126.
24 B. Ohtani, S.-W. Zhang, S. Nishimoto and T. Kagiya, *J. Chem. Soc., Faraday Trans.*, 1992, **88**, 7, 1049–1053.
25 M. H. Mahibi and H. Vosooghian, *J. Photochem. Photobiol., A*, 2005, **174**, 1, 45–52.
26 H.-S. Roh, D. L. King and Y. Wang, *Prepr. - Am. Chem. Soc., Div. Pet. Chem.*, 2004, **49**, 2.
27 G. D. Wilk, R. M. Wallace and J. M. Anthony, *J. Appl. Phys.*, 2001, **89**, 5243–75.
28 M. Kadoshima, M. Hiratani, Y. Shimamoto, Y. Miki, S. Kimura and T. Nabatame, *Thin Solid Films*, 2003, **424**, 224.
29 A. N. Luiten, M. E. Tobari, J. Krupka, R. Woode, E. N. Ivanov and A. G. Mann, *J. Phys. D: Appl. Phys.*, 1998, **31**, 1383–1391.
30 J. E. G. J. Wijnhoven and W. L. Vos, *Science*, 1998, **281**, 802–804.
31 C. Singh, M. S. P. Shaffer and A. H. Windle, *Carbon*, 2003, **41**, 359–368.
32 S. Vargas, R. Arroyo, E. Haro and R. Rodriguez, *J. Mater. Res.*, 1999, **14**, 10, 3932–3937.